

Dynamical effects of the neutrino gravitational clustering at PLANCK angular scales

L.A. Popa¹, C. Burigana and N. Mandolesi

IASF/CNR, Istituto di Astrofisica Spaziale e Fisica Cosmica, Sezione di Bologna,
Consiglio Nazionale delle Ricerche, Via Gobetti 101, I-40129 Bologna, Italy

Received _____; accepted _____

Submitted to ApJ, 14 March 2002.

¹further address: Institute of Space Sciences, Bucharest-Magurele, R-76900, Romania

ABSTRACT

We study the CMB anisotropy induced by the non-linear perturbations in the massive neutrino density associated to the non-linear gravitational clustering process. By using N-body simulations, we compute the imprint left by the gravitational clustering on the CMB anisotropy power spectrum for all non-linear scales taking into account the time evolution of all non-linear density perturbations, for a flat Λ CDM model consistent with LSS data and latest CMB measurements for different neutrino fractions f_ν corresponding to a neutrino total mass in the range allowed by the neutrino oscillation and double beta decay experiments.

We find that the non-linear time varying potential induced by the gravitational clustering process generates metric perturbations, leaving a decrease in the CMB anisotropy power spectrum of amplitude $\Delta T/T \approx 10^{-6}$ for angular resolutions between ~ 4 and 20 arcminutes, depending on the cluster mass scale and the neutrino fraction f_ν . We find also that the consistency among BOOMERANG, MAXIMA-1 and DASI CMB angular power spectra and the errors on most of the cosmological parameters improve when the non-linear effects induced by the gravitational clustering are taken into account. Our results show that, for a neutrino fraction in agreement with that indicated by the astroparticle and nuclear physics experiments and a cosmological accreting mass comparable with the mass of known clusters, the angular resolution and sensitivity of the CMB anisotropy measurements from the PLANCK satellite will allow the detection of the dynamical effects of the gravitational clustering.

This work has been done in the framework of the PLANCK LFI activities.

Subject headings: Cosmology: cosmic microwave background – large scale

structure – dark matter – Elementary particles

1. Introduction

The study of the Cosmic Microwave Background (CMB) radiation holds the key of understanding the seeds of the cosmological structures of our present universe, enabling the measurements for most of the important cosmological parameters. The new generation of CMB experiments as MAP² and PLANCK³ will achieve enough precision to reveal more cosmological information on the structure formation process up to arcminute angular scales. Inside the horizon, the acoustic, Doppler, gravitational redshift and photon diffusion effects combine to determine the angular power spectrum of CMB primary anisotropies. The secondary effects generated between the recombination and the present can also alter the CMB anisotropy, providing more details on the evolution of the structures and less robust constraints on the background parameters (Hu, Sugiyama & Silk 1997). The secondary effects are basically divided into two categories: gravitational effects from metric distortions and rescattering effects from reionization. The gravitational effects include the early integrated Sachs-Wolfe (ISW) effect (see e.g. Hu & Sugiyama 1995), the late ISW effect (Kofman & Starobinskii 1985), the Rees-Sciama effect (Rees & Sciama 1968) as well as the contribution from gravitational waves and gravitational lensing (Blanchard & Schneider 1987, Cole & Efstathiou 1989). The rescattering effects both erase the CMB primary anisotropies and generates secondary anisotropies through the Doppler effect (Kaiser 1984). Secondary anisotropies at very small scales can be more efficiently generated by higher order contributions than by the Doppler effect. They include the Vishniac effect (Ostriker

²<http://map.gsfc.nasa.gov>

³<http://astro.estec.esa.nl/Planck>

& Vishniac 1986, Vishniac 1987) associated to linear perturbations in the baryon density, spatial inhomogeneities of the ionization fraction (Aghanim & Forni 1999, Gruzinov & Hu 1988) and the kinematic and thermal Sunyaev-Zel’dovich effect from clusters (Sunyaev & Zel’dovich 1972).

In this paper we study the CMB secondary anisotropies induced by the non-linear perturbations in the massive neutrino density associated to the non-linear gravitational clustering. The dynamical role of the massive neutrinos in the gravitational clustering process was extensively considered in the literature (Tremaine & Gunn 1979, Bond, Efstathiou & Silk 1980, Bond & Szalay 1983, Ma 2000, Primack & Gross 2000). The extent to which the massive neutrinos can cluster gravitationally depends on their mass and the parameters of the fiducial cosmological model describing the present universe.

The atmospheric neutrino experiments (Fukuda et al. 1998, Ambrosio et al. 1998) provides strong evidences of neutrino oscillations implying a non-zero neutrino mass with a lower limit in the range $0.04 - 0.08$ eV. The latest measurements of the contribution of the double beta decay to the neutrino mass matrix (Klapdor-Kleingrothaus 2001) placed an upper limit on the neutrino mass of $m_\nu \leq 0.26$ eV. The direct implication of these results is the non-negligible contribution of the hot dark matter (HDM) to the total mass density of the universe and the existence of three massive neutrino flavors (i.e. a density parameter $\Omega_\nu h^2 \approx \sum_{i=1}^3 m_i / 93 \text{ eV}$, where $h = H_0 / 100 \text{ Km s}^{-1} \text{ Mpc}^{-1}$ is the dimensionless Hubble constant), that is also required by the consistency between the CMB anisotropy at the small scales with the Large Scale Structure (LLS) of the universe derived by the galaxy surveys (e.g. Scott & White 1994; White et al. 1995; Primack et al. 1995; Gawiser & Silk 1998).

Evidences has been accumulated that we live in a low matter density universe (see e.g. Fukugita, Liu & Sugiyama 1999 and the references therein). Indications like Hubble diagram of Type 1a supernovae (Riess et al. 1998, Perlmutter et al. 1998) and the acoustic

peak distribution in the CMB anisotropy power spectra (Hancock et al. 1998, Efstathiou et al. 1999), point to a universe close to be flat because of a significant cosmological constant Λ possibly due to a large vacuum energy density. The analysis of the latest CMB anisotropy data including BOOMERANG (Netterfield et al. 2001), DASI (Halverson et al. 2001) MAXIMA-1 (Lee et al. 2001), and CBI (Padin et al. 2001), alone or complemented with other cosmological data sets involving galaxy clustering and Lyman Alpha Forest (Wang, Tegmark & Zaldarriaga 2001) point also to a Λ -dominated low matter density universe with neutrino masses in the range of $0.04 - 4.4$ eV.

It is therefore worthwhile to investigate the effects of the gravitational clustering on the CMB angular power spectrum in Λ cosmological models involving a HDM component (Λ CHDM) in the form of three massive neutrino flavors with the total mass in eV range.

The linear perturbation theory describes accurately the growth of density fluctuations from the early Universe until a redshift $z \sim 100$ (see the CMBFAST code by Seljak & Zaldarriaga 1996). The solution involves the integration of coupled and linearized Boltzmann, Einstein and fluid equations (Ma & Bertschinger 1995) that describes the time evolution of the metric perturbations in the perturbed density field and the time evolution of the density fields in the perturbed space-time for all the relevant species (e.g., photons, baryons, cold dark matter, massless and massive neutrinos). At lower redshifts the gravitational clustering becomes a non-linear process and the solution relies on numerical simulations.

Through numerical simulations, we compute the CMB anisotropy in the non-linear stages of the evolution of the universe when clusters and superclusters of galaxies start to form producing a non-linear gravitational potential varying with time. By using a standard particle-mesh method (Efstathiou & Eastwood 1991, Hockney & Eastwood 1981), we analyze the imprint of the dynamics of the neutrino gravitational clustering on the CMB anisotropy power spectrum in a flat Λ CHDM model (see Tab. 1) with $\Omega_m=0.38$, $\Omega_\Lambda=0.62$,

$H_0=62 \text{ Km s}^{-1} \text{ Mpc}^{-1}$ and different neutrino fractions $f_\nu = \Omega_\nu/(\Omega_b + \Omega_{cdm})=0.06, 0.11, 0.16$ corresponding to $\Omega_\nu=0.022$ ($m_\nu=0.78\text{eV}$), 0.037 ($m_\nu=1.35 \text{ eV}$), 0.053 ($m_\nu=1.89\text{eV}$). We assume three massive neutrino flavors, a primordial power spectrum with the scalar spectral index $n_s=0.98$, an optical depth to the last scattering $\tau=0.12$ and neglect the contribution from the tensorial modes (gravitational waves). This model is consistent with the LSS data and the CMB anisotropy latest measurements, allowing in the same time a pattern of neutrino masses consistent with the results from neutrino oscillation and double beta decay experiments.

In Section 2 we discuss the physical aspects related to the dynamics of the neutrino gravitational infall due to non-linear clustering. Section 3 presents the N-body simulations used for the computation of the power spectra of the CMB temperature fluctuations. In Section 4 we make estimates of the dynamics of the gravitational clustering imprinted on the CMB angular power spectra by using the latest anisotropy measurements in the field. Finally, we draw our conclusions in Section 5.

Throughout the paper we use the system of units in which $\hbar = c = k_B = 1$.

Table 1: Cosmological parameters assumed in this study for the considered fiducial flat Λ CHDM model.

Ω_{tot}	f_ν	Ω_{cdm}	Ω_b	Ω_Λ	Ω_ν	$m_\nu(\text{eV/}\text{flavor})$	h	n_s	τ
1	0.06	0.308	0.05	0.62	0.0216	0.26	0.62	0.98	0.12
1	0.11	0.293	0.05	0.62	0.0373	0.45	0.62	0.98	0.12
1	0.16	0.277	0.05	0.62	0.0522	0.63	0.62	0.98	0.12

2. The neutrino gravitational infall

In the expanding universe, neutrinos decouple from the other species when the ratio of their interaction rate to the expansion rate falls below unity. For neutrinos with masses in the eV range the decoupling temperature is $T_D \sim 1\text{MeV}$, occurring at a redshift $z_D \sim 10^{10}$ (Freese, Kolb & Turner 1983). At this time neutrinos behave like relativistic particles with a pure Fermi-Dirac phase-space distribution:

$$f_\nu(q, a) = \frac{1}{e^{E_\nu/T_\nu+1}}, \quad E_\nu = \sqrt{q^2 + a^2 m_\nu^2}, \quad (1)$$

where: \vec{q} is the neutrino comoving momentum, $\vec{q} = a\vec{p}$, \vec{p} being the neutrino 3-vector momentum, E_ν is the energy of neutrino with mass m_ν and a is the cosmic scale factor ($a_0=1$ today).

As neutrinos are collisionless particles, they can significantly interact with photons, baryons and cold dark matter particles only via gravity. The neutrino phase space density is constrained by the Tremaine & Gunn (1979) criterion that put limits on the neutrino energy density inside the gravitationally bounded objects. Following Tremaine & Gunn criterion it is shown that in the cosmological models involving a HDM component (the CHDM models) the compression fraction of neutrinos through a cluster $f(r) = \rho_\nu/\rho_{cdm}$ (where r is the cluster radius) never exceeds the background ratio Ω_ν/Ω_{cdm} (Kofman et al. 1996). Because the formation of galaxies and clusters is a dynamical time process, the differences introduced in the gravitational potential due to neutrino gravitational clustering generate metric perturbations that affect the evolution of the density fluctuations of all the components of the expanding universe. Fig. 1 presents the evolution of the projected mass distributions of cold dark matter plus baryons and neutrinos obtained from numerical simulations at few redshift values z (see Section 2 for details of the simulations). One can see that neutrinos are accreted by the cold dark matter and baryons, contributing in the dynamic way to the gravitational clustering process.

Neutrinos cannot cluster via gravitational instability on distances below the free-streaming distance R_{fs} (Bond, Efstathiou & Silk 1980, Bond & Szalay 1983, Ma 2000). The neutrino free-streaming distance is related to the causal comoving horizon distance $\eta(a)$ through (Dodelson, Gates & Stebbins 1996):

$$R_{fs}(a) = \frac{1}{k_{fs}} = \frac{\eta(a)}{\sqrt{1 + (a/a_{nr})^2}} \text{Mpc}, \quad \eta(a) = \int_0^a \frac{da}{a^2 H(a)}, \quad (2)$$

where a_{nr} is the value of the scale factor when massive neutrinos start to become non-relativistic ($a_{nr} = (1 + z_{nr})^{-1} \approx 3k_B T_{\nu,0}/m_\nu c^2$) and $H(a)$ is the Hubble expansion rate:

$$H^2(a) = \frac{8\pi G}{3} [\Omega_m/a^3 + \Omega_r/a^4 + \Omega_\Lambda + \Omega_k/a^3]. \quad (3)$$

In the above equation G is the gravitational constant, $\Omega_m = \Omega_b + \Omega_{cdm} + \Omega_\nu$ is the matter energy density parameter, Ω_b , Ω_{cdm} , Ω_ν being the energy density parameters of baryons, cold dark matter and neutrinos, Ω_r is the radiation energy density parameter that includes the contribution from photons and relativistic neutrinos, Ω_Λ is the vacuum energy density parameter, $\Omega_k = 1 - \Omega_m - \Omega_\Lambda$ is the energy density parameter related to the curvature of the universe and $a = (1 + z)^{-1}$ is the cosmic scale factor.

R_{fs} defines the minimum linear dimension that a neutrino perturbation should have in order to survive the free-streaming. In the spherical approximation, the minimum comoving mass of a perturbation that should contain clusterized neutrinos, corresponds to (Kolb & Turner 1990):

$$M(R_{fs}) = \frac{\pi}{6} R_{fs}^3 \rho_m \approx 1.5 \times 10^{11} (\Omega_m h^2) (R_{fs}/\text{Mpc})^3 h^{-1} M_\odot,$$

where Ω_m is the matter energy density parameter.

We show in Fig. 2 the dependence of the causal horizon distance $\eta(a)$, the neutrino free-streaming distance R_{fs} , [panel a)] and of the mass $M(R_{fs})$ [panel b)] on the cosmic scale factor. The cosmological model is the Λ CHDM model with different neutrino fractions f_ν . One can see that at early times, when neutrinos are relativistic, the free-streaming distance

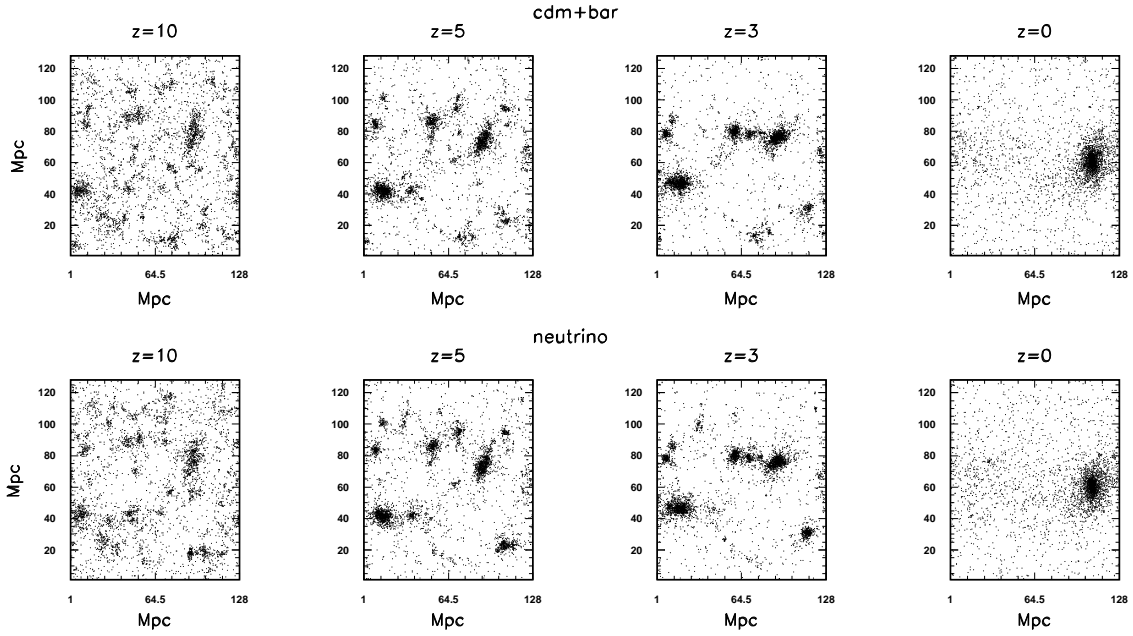


Fig. 1.— The evolution with the redshift of the projected mass distributions of cold dark matter plus baryons (upper row) and neutrinos (lower row) obtained from numerical simulation of 128^3 cold dark matter plus baryons (the total mass of $8 \times 10^{16} M_\odot$) and 10×128^3 neutrinos (the total mass of $4.8 \times 10^{18} M_\odot$) in a box of size 128 Mpc, for the Λ CHDM model with the neutrino fraction $f_\nu = 0.16$.

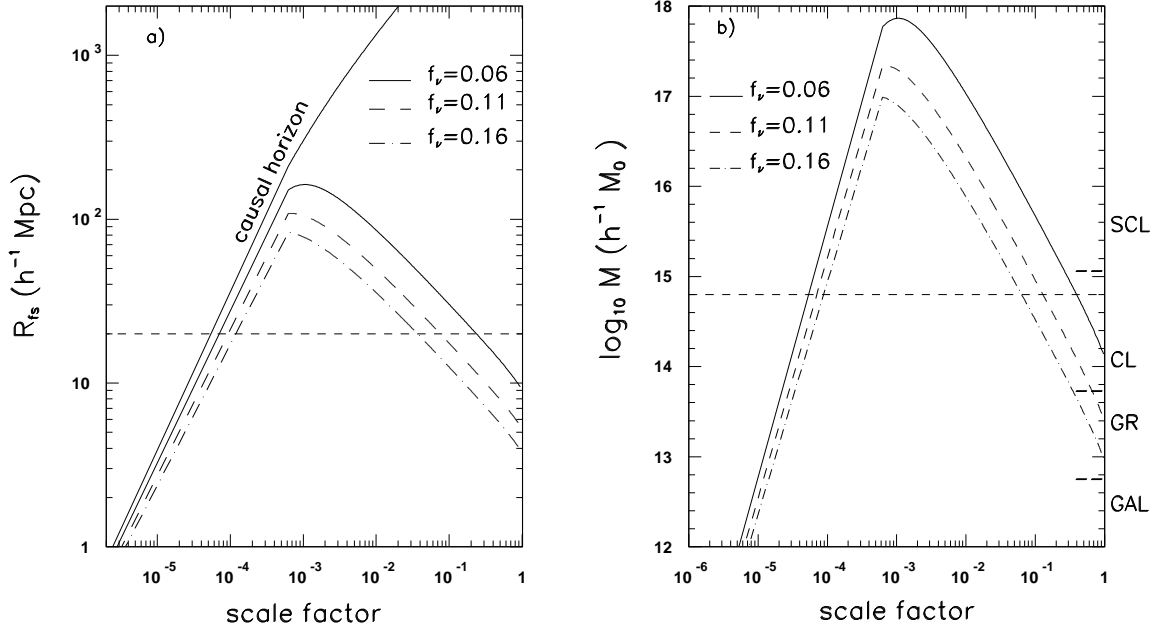


Fig. 2.— Panel a): dependence of the neutrino free-streaming distance R_{fs} on the scale factor. We show also a specific scale, $\lambda = 20 h^{-1} \text{ Mpc}$, constant in comoving coordinates (horizontal dashed line) and the evolution with the scale factor of the causal horizon distance for our cosmological models. Panel b): dependence on the scale factor of the mass $M(R_{fs})$ of the perturbation at the scale R_{fs} . We show also the mass of the perturbation at the scale λ (horizontal dashed line) and indicate the typical mass ranges for galaxies (GAL), groups (GR), clusters (CL) and superclusters (SCL).

is approximately the causal horizon distance. After neutrinos become non-relativistic ($a_{nr} \sim 10^{-4}$ for our cosmological models) the free-streaming distance decreases with time, becoming smaller than the causal horizon distance. The time behaviors of R_{fs} and $M(R_{fs})$ show that neutrino can cluster gravitationally on increasingly smaller scales at latter times. If the causal horizon $\eta(a)$ is large enough to encompass the wavelength λ , the neutrino gravitational infall perturbs the growth of the perturbations for this mode, leaving imprints in the CMB angular power spectrum. Perturbations on scales $\lambda < R_{fs}$ ($k > k_{fs}$) are damped due to the neutrino free-streaming while the perturbations on scales $\lambda > R_{fs}$ ($k < k_{fs}$) are affected only by gravity.

3. CMB anisotropy power spectrum in presence of neutrino gravitational clustering

Based on the anisotropy produced by a single cluster modeled in the spherical approximation, earlier estimates of the CMB anisotropy produced by the non-linear density perturbations (Martinez-Gonzalez & Sanz 1992) give only upper limits on degree angular scales.

As the anisotropy produced by the non-linear density perturbations depends on the time variations of the spatial gradients of the gravitational potential produced by different components (cold dark matter, baryons, neutrinos), we calculate the CMB anisotropy in the presence of the gravitational clustering by using N-body simulation in large boxes with the side of 128 Mpc, that include all non-linear scales used in the computation of the CMB anisotropy power spectrum from $\lambda_{min} \approx 12\text{Mpc}$ ($k_{max} \approx 0.52\text{Mpc}^{-1}$) to $\lambda_{max} \approx 110\text{Mpc}$ ($k_{min} \approx 0.06\text{Mpc}^{-1}$), taking into account the time evolution of all non-linear density perturbations influencing the CMB power spectrum (see also Fig. 1). One should note that λ_{max} corresponds to the comoving horizon size at the matter-radiation equality for our

cosmological models ($\lambda_{eq} \approx 16 \Omega_m^{-1} h^{-2} \text{Mpc}$). The non-linear structures are assumed to be formed by two components: cold dark matter plus baryons and neutrinos in the form of three massive neutrino flavors, both components evolving in the gravitational field created by themselves. For the purpose of this work we neglect the hydrodynamical effects. This approach is justified as the contributions to the CMB anisotropy of the hot baryonic gas is proved to be negligible (Quilis, Ibanez & Saez 1995).

3.1. Basic equations

In the Newtonian limit, the neutrino gravitational clustering can be described as a deviation from the background by a potential Φ given by the Poisson equation:

$$\nabla^2 \Phi(\vec{r}, a) = 4\pi G a^2 \rho_m(a) \delta_m(\vec{r}, a), \quad (4)$$

where \vec{r} is the position 3-vector, $\rho_m(a)$ is the matter density and $\delta_m(\vec{r}, a)$ is the matter density fluctuation; $\delta_m = \delta_b + \delta_c + \delta_\nu$, where δ_c , δ_b and δ_ν are the density fluctuations for cold dark matter particles, baryons and neutrinos.

The equations governing the motion of each particle species (cold dark matter plus baryons and neutrinos) in the expanding universe are given by (Kates, Kotok & Klypin 1991, Gleb & Bertshinger 1994):

$$\frac{d\vec{q}}{da} = -a H(a) \vec{\nabla} \Phi, \quad \frac{d\vec{r}}{da} = \vec{q} (a^3 H(a))^{-1}, \quad (5)$$

where \vec{q} is the comoving momentum and $H(a)$ is the Hubble expansion rate given by the equation (3).

The Newtonian description given by the equations (4)–(5) applies in the limit of the weak gravitational field if, at each time step, the size of the non-linear structures is much smaller than the causal horizon size (the background curvature is negligible).

3.2. N-body simulations

The cosmological models involving massive neutrinos show a characteristic scale-dependence of the perturbation growth rates (Ma 1996, Hu & Eisenstein 1998, Popa, Burigana, Mandolesi 2001). We evolve the system of baryons plus cold dark matter particles and neutrinos according to the equations (4) and (5) for the non-linear scales involved in the computation of the CMB anisotropy ($0.06\text{Mpc}^{-1} \leq k \leq 0.52\text{Mpc}^{-1}$), starting from the beginning of the non-linear regime of cold dark matter plus baryons component.

The initial positions and velocities of neutrinos and baryons plus cold dark matter particles are generated at each spatial wave number k from the corresponding matter density fluctuations power spectra at the present time by using the Zel’dovich approximation (Zel’dovich 1970). The matter power spectra was normalized on the basis of the analysis of the local cluster X-ray temperature function (Eke, Cole & Frenk 1996). We performed simulations with 128^3 cold dark matter plus baryon particles and 10×128^3 neutrinos. The neutrinos and the baryons plus cold dark matter particles was randomly placed on 128^3 grids, with comoving spacing r_0 of $0.5 \text{ h}^{-1}\text{Mpc}$. The high number of neutrinos and this comoving spacing ensure a precision high enough for a correct sampling of the neutrino phase space distribution (Popa, Burigana, Mandolesi 2001).

According to the Zel’dovich approximation, the perturbed comoving position of each particle $\vec{r}(\vec{r}_0, a)$ and its peculiar velocity $\vec{v}(\vec{r}_0, a)$ are related to the fluctuations of the density field $\delta\rho(\vec{r}_0, a, k)$ through:

$$\begin{aligned} \vec{r}(\vec{r}_0, k, a) &= \vec{r}_0 + D(k, a)\vec{d}(\vec{r}_0), \quad \vec{v}(\vec{r}_0, k, a) = \dot{D}(k, a)\vec{d}(\vec{r}_0), \\ \vec{\nabla}\vec{d}(\vec{r}_0) &= D^{-1}(k, a)\delta\rho(\vec{r}_0, k, a), \end{aligned} \tag{6}$$

where \vec{r}_0 is the coordinate corresponding to the unperturbed comoving position, $\vec{d}(\vec{r}_0)$ is the displacement field and $D(k, a)$ is the growth function of perturbations corresponding to each cosmological model.

At each wave number k used in the computation of the CMB anisotropy we compute the perturbed particles comoving positions and peculiar velocities at the beginning of the non-linear regime a_{nl} , by using the set of equations (6). We assign to each particle a momentum according to the growth function, when the power of each mode is randomly selected from a Gaussian distribution with the mean accordingly to the corresponding power spectrum (Hoffman & Ribak 1991, Ganon & Hoffman 1993, Bertschinger 1995). In the computation of the set of equation (6) we consider only the growing modes, the non-linear power spectra up to $k_{max} = 6.28 \text{ h Mpc}^{-1}$, and neglect the contribution of the redshift distortions.

We present in Fig. 3 the dependence on the spatial wave number k of the scale factor a_{nl} for each component. One can see from Fig. 3 that neutrinos (panel a) enter in the non-linear regime later than cold dark matter particles and baryons (panel b). Thus, the neutrino halo of the cluster starts to form after the cold dark matter plus baryon halo is advanced in the non-linear stage, causing the accretion of neutrinos from the background.

At each spatial wavenumber k we evolve the particles positions and velocities according to the set of equations (4)-(5). We start this process from the scale factor a_{nl}^c at which cold dark matter particles plus baryons start to enter in the non-linear regime. At each time step, the density on the mesh is obtained from the particle positions using the Cloud-in-Cell method and equation (4) is solved by using 7-point discrete analog of the Laplacian operator and the FFT technique (Klypin & Holtzman 1997). The particle positions and velocities are then advanced in time with a time step da required by the computation of the CMB anisotropy power spectra. The system of particles was evolved until the scale factor a_{st} when, according to the virial theorem (Peacock 2001), it reaches the equilibrium. The virial theorem states that a system of particles evolving in the gravitational field achieves its equilibrium state when the time averaged kinetic energy E_k and the potential energy E_p of the system are related through: $E_p = -2E_k$. We present in panel a) of Fig. 4 the evolution

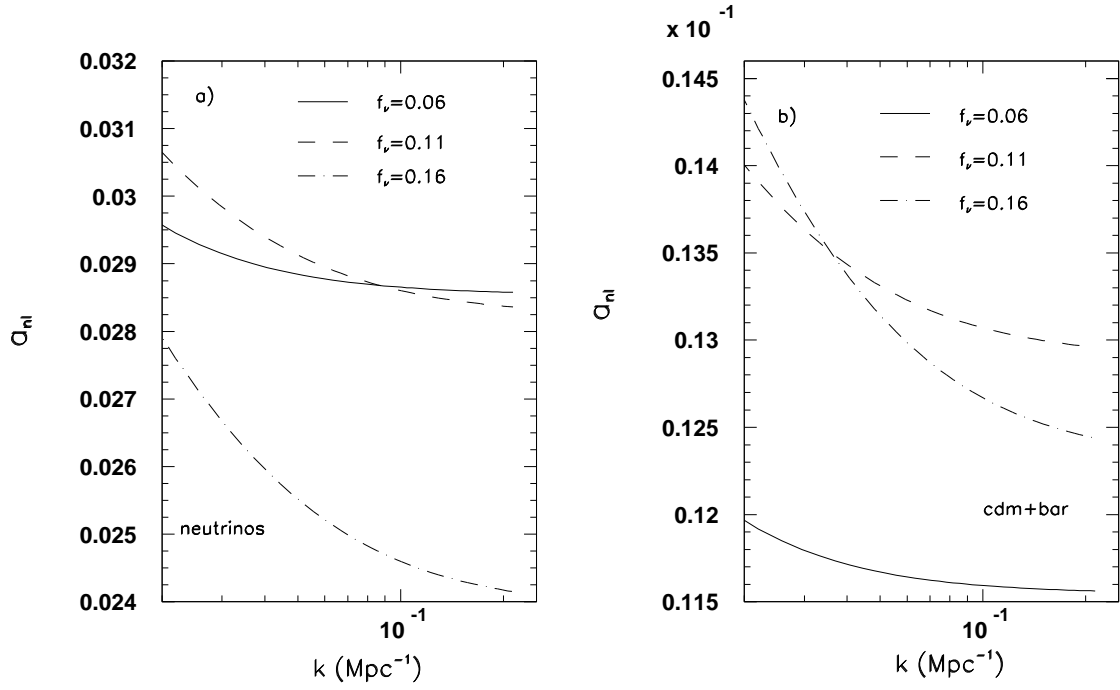


Fig. 3.— The scale dependence of a_{nl} for neutrinos (panel a) and baryons plus cold dark matter particles (panel b).

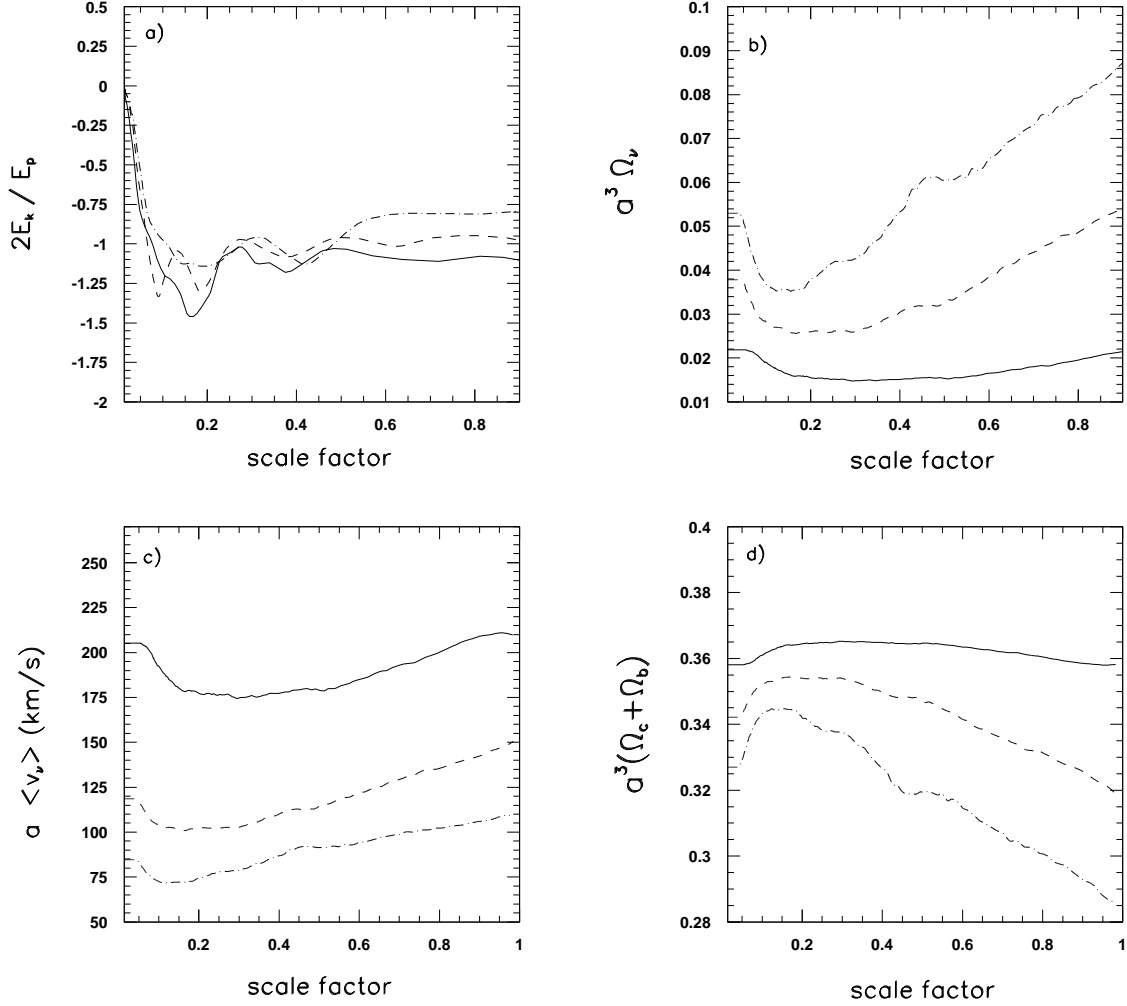


Fig. 4.— The evolution with the scale factor a of: the ratio of the kinetic energy (E_k) and potential energy (E_p) for the system of particles considered in the simulation [Panel a)]; the neutrino comoving energy density parameter [Panel b)]; the neutrino averaged comoving velocity [Panel c)]; the comoving energy density parameter of cold dark matter plus baryons [Panel d)]. All plots are obtained for mode $k = 0.06 \text{ Mpc}^{-1}$ and different neutrino fractions: $f_\nu = 0.06$ (solid lines), 0.11 (dashed lines), 0.16 (dash-dotted lines).

of the ratio $2E_k/E_p$ with the scale factor, for different neutrino fractions. In all cases the system of particles achieves the equilibrium condition at $a_{st} \approx 0.4$ ($z \approx 1.5$).

The neutrino momentum field obtained at each wave number k and scale factor a was sampled in fixed equispaced points (we use here $N_{q_{max}}=50$) and normalized to the neutrino total number ($N_{part} = 10 \times 128^3$ in the current simulation). In this way we obtained the time evolution of the full phase space neutrino distribution function by including the perturbation from the initial phase space distribution due to the non-linear evolution of the gravitational field.

At each time step the neutrino energy density and pressure are obtained as:

$$\rho_\nu(a) = \frac{T_\nu^4(a)}{2\pi^2} \int_0^\infty dq q^2 E_\nu(a) f_\nu(a, q), \quad p_\nu(a) = \frac{T_\nu^4(a)}{2\pi^2} \int_0^\infty dq \frac{q^2}{E_\nu(a)} f_\nu(a, q), \quad (7)$$

where: $T_\nu(a)$ is the neutrino temperature and $E_\nu(a)$, $f_\nu(a, q)$ are the neutrino comoving energy and the neutrino phase space distribution function as given by the eq. (1).

Panel b) of Fig. 4 presents the evolution with the scale factor of the neutrino comoving energy density parameter $a^3\Omega_\nu$ obtained for different neutrino fractions. To better understand the time behavior of the neutrino energy density parameter, we present in the panel c) of the same figure the time evolution of the averaged neutrino comoving velocity $a < v_\nu >$.

When cold dark matter particles plus baryons start to evolve in the non-linear regime, neutrinos are still in linear regime, having a pure Fermi-Dirac phase space distribution. As the system evolves in time, its potential energy start to increase, causing perturbations of the neutrino phase space distribution from the pure Fermi-Dirac distribution. Fig. 5 presents the neutrino comoving momentum distribution functions computed at few different time steps. For comparison, we plot also a pure Fermi-Dirac distribution. At early stages, when $a_{nl}^c < a < a_{nl}^\nu$ (a_{nl}^ν is the value of the scale factor when neutrinos start to enter in the non-linear regime) neutrinos are not accreted by the non-linear structures created by the

cold dark matter and baryons as their typical averaged velocity $\langle v_\nu \rangle$ is too large:

$$\langle v_\nu \rangle \approx 160 a^{-1} \left(\frac{1\text{eV}}{m_\nu} \right) \text{ Km/s.}$$

As the potential energy of the system increases, the neutrino averaged comoving velocity, the comoving momentum and the comoving energy density are decreased until the neutrino averaged velocity drops below the averaged velocity dispersion of cold dark matter and baryons. Then, neutrinos start to fall in the gravitational potential wells created by the cold dark matter and baryons and their kinetic energy start to increase. Consequently, the averaged neutrino comoving velocity, the comoving momentum and the comoving energy density tends to increase as the system approaches its equilibrium state.

As the consequence of the matter energy density conservation each time step, the comoving energy density of cold dark matter particles plus baryons shows an opposite time dependence, as presented in panel d) of Fig. 4.

3.3. Imprints on CMB anisotropy power spectrum

In this section we compute the imprints of the dynamics of the neutrino gravitational clustering on the CMB anisotropy power spectrum.

The neutrino gravitational clustering can affect both the homogeneous and the inhomogeneous components of the gravitational field. The changes in the homogeneous component of the gravitational field are determined by the changes of the energy density of neutrinos and cold dark matter particles plus baryons. They affect the Hubble expansion rate, the sound horizon distance and the neutrino free-streaming distance [see equations (3) and (4)]. The changes in the inhomogeneous component of the gravitational field are determined by the changes in the energy density for all matter components and the changes in the neutrino phase space distribution function. They affect (see equations (21) from Ma & Bertschinger 1995) the growth of the energy density perturbations of cold dark matter, baryons, photons,

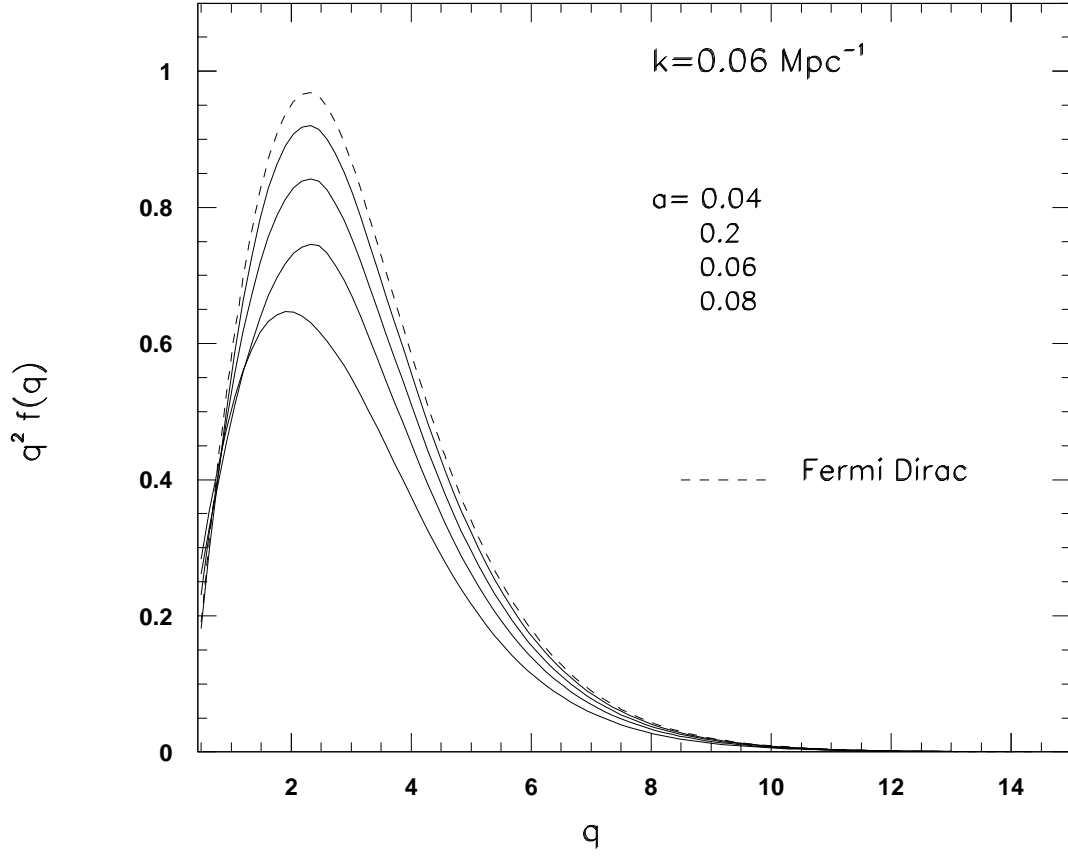


Fig. 5.— The neutrino comoving momentum distribution function computed at few different time steps. From the top to the bottom the scale factor is $a = 0.04, 0.2, 0.06, 0.08$. The dashed line represents the pure Fermi-Dirac distribution function. All distributions are obtained for the mode $k=0.06\text{Mpc}^{-1}$ and for the neutrino fraction $f_\nu=0.06$

massive and massless neutrinos. In the linear regime ($a \leq a_{nl}^c$, for each perturbation mode k we compute the energy density perturbations, the pressure, the energy flux and the shear stress for all the components in the synchronous gauge by using the CMBFAST code.

In the non-linear regime ($a \geq a_{nl}^c$), we compute the neutrino phase space distribution function, the energy density of cold dark matter, baryons and neutrinos at each perturbation mode $k \geq k_{min}$, as described in the previous section. Then, following the same procedure implemented in the CMBFAST code, we compute in the synchronous gauge the perturbations of the energy density, the pressure, the energy flux and the shear stress for all the components of our cosmological model.

Panel a) of Fig. 6 presents the evolution with the scale factor of the energy density perturbations of different components in the non-linear regime, for the mode $k = 0.06 \text{ Mpc}^{-1}$ (solid lines). For comparison, we plot also (dashed lines) the energy density perturbations of the different components obtained for the same mode k in absence of the gravitational clustering (linear regime). The cosmological model has a neutrino fraction $f_\nu = 0.06$. One can see that the neutrino gravitational clustering affects the growth of the energy density perturbations for all components. Panel b) of Fig. 6 presents the evolution with the scale factor of the scalar potential Ψ of the conformal Newtonian gauge line element, that plays the role of the gravitational potential in the Newtonian limit (Bardeen 1980, Kodama & Sasaki 1984), by including (solid line) or not (dashed line) the effect of neutrino gravitational clustering. [For the transformation relation between the scalar potentials of the synchronous gauge and conformal Newtonian gauge see equation (18) of Ma & Bertschinger (1995)].

Fig. 7 presents our computed CMB anisotropy power spectra in the presence of the neutrino gravitational clustering. The cosmological model is the Λ CHDM model having different neutrino fractions. We note that the far-IR source clustering contribution to the

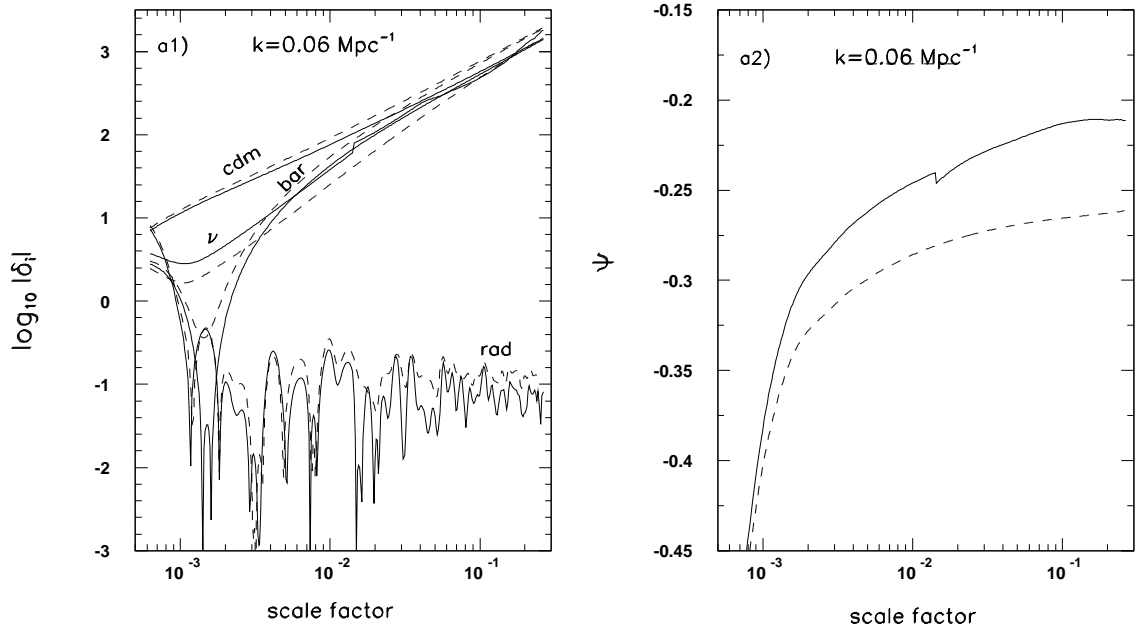


Fig. 6.— Panel a): time evolution of the energy density perturbations of the different components as computed by including the gravitational clustering (solid lines) and by neglecting the gravitational clustering (dashed lines): cold dark matter (cdm), baryons (bar), massive neutrinos (ν), and massless neutrinos plus photons (rad). Panel b): the same as in panel a), but for the time evolution of the gravitational field [$k=0.06\text{Mpc}^{-1}$ and $f_\nu = 0.06$].

extragalactic foreground fluctuations may contribute significantly to the angular power spectrum at $\ell \gtrsim 100$ (Magliocchetti et al. 2001). On the other hand, this effect may be important also about the first Doppler peak and shows a remarkable frequency dependence, while the neutrino gravitational clustering effect decreases the power of the secondary Doppler peaks with respect to that of the first Doppler peak and does not depend on the frequency. Therefore, an accurate CMB anisotropy experiment with a wide frequency coverage, like PLANCK, can in principle clearly resolve the combined effect of these two contributions.

As we have shown before, the difference in the evolution of a perturbation mode k depends on how this mode relates to the neutrino free-streaming wave number k_{fs} . Considering that our simulation at each time step is a sample of the evolution of the matter in the non-linear regime, we study the imprint of the gravitational clustering on the CMB anisotropy power spectrum by smoothing the density field obtained from simulation at each time step with a filter with the scale R_{fs} corresponding to the cluster mass value $M(R_{fs})$. For each non-linear mode k only the perturbations with the mass $M \leq M(R_{fs})$ are taken into account for the computation of the CMB anisotropy power spectrum.

Fig. 8 presents our computed CMB anisotropy power spectra obtained when different filtering mass values $M(R_{fs})$ are considered. It is usual to use the Coma cluster as the mass normalization point ($M_{\text{Coma}} = 1.45 \times 10^{15} h^{-1} M_{\odot}$); for the Coma cluster we assume a richness $\mathcal{A}_{\text{Coma}}=106$. According to Kashlinsky (1998), the relation between the mass of the perturbation and the richness \mathcal{A} of the corresponding cluster can be written in the form:

$$M = M_{\text{Coma}} \frac{\mathcal{A}}{\mathcal{A}_{\text{Coma}}} = 1.45 \times 10^{15} \left(\frac{\mathcal{A}}{106} \right) h^{-1} M_{\odot}.$$

By comparing the angular power spectra obtained including or not the neutrino gravitational clustering effect, we find a decrease of the CMB angular power spectrum induced by the neutrino gravitational clustering of $\Delta T/T \approx 10^{-6}$ for angular resolutions between ~ 4 and 20 arcminutes, depending on the cluster mass and neutrino fraction f_{ν} .

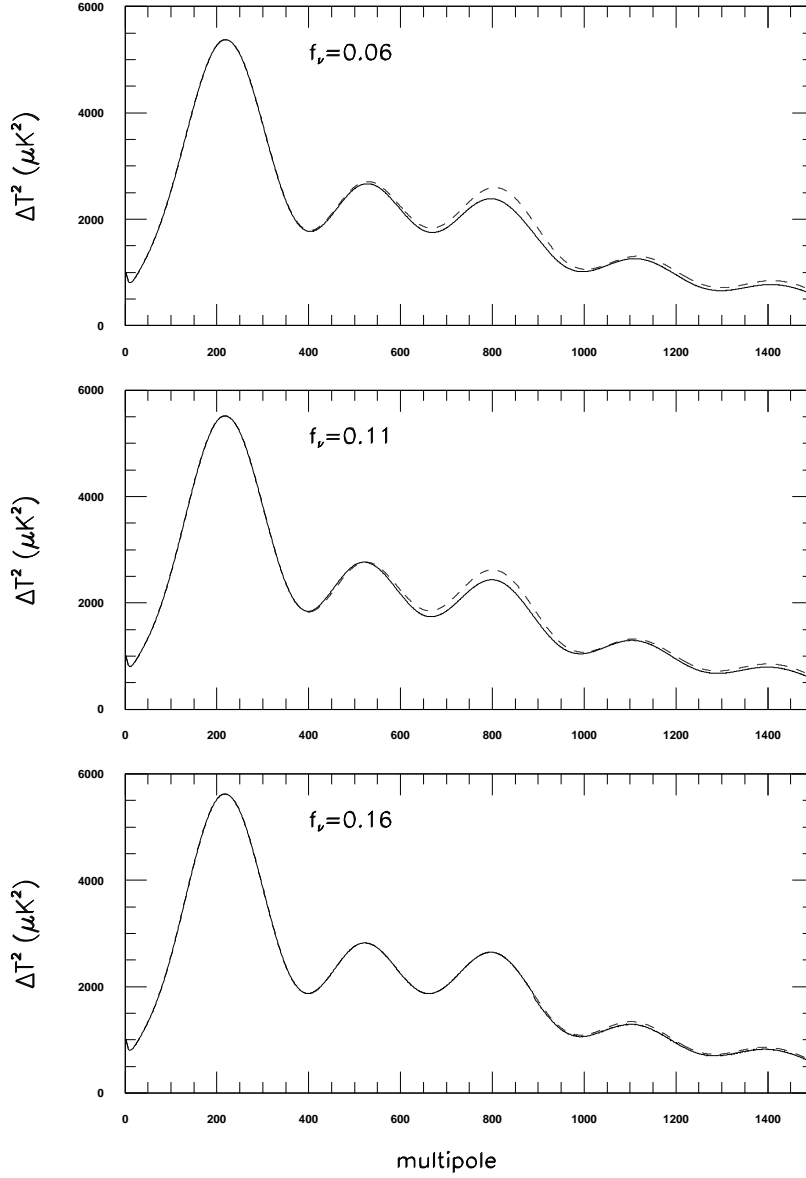


Fig. 7.— The CMB anisotropy power spectra computed in the presence of the neutrino gravitational clustering (solid lines). In each panel we show also the fiducial Λ CDM cosmological model without including the neutrino gravitational clustering (dashed line), with: $\Omega_m = 0.68$, $\Omega_\Lambda = 0.62$, $h = 0.62$, $n_s = 0.98$, $\tau = 0.12$, three massive neutrino flavors and different neutrino fractions ($f_\nu=0.06, 0.11, 0.16$, from the top to the bottom). As usual, we express the CMB anisotropy power spectrum in terms of $\Delta T^2 = C_\ell \ell(\ell+1)/2\pi$. See also the text.

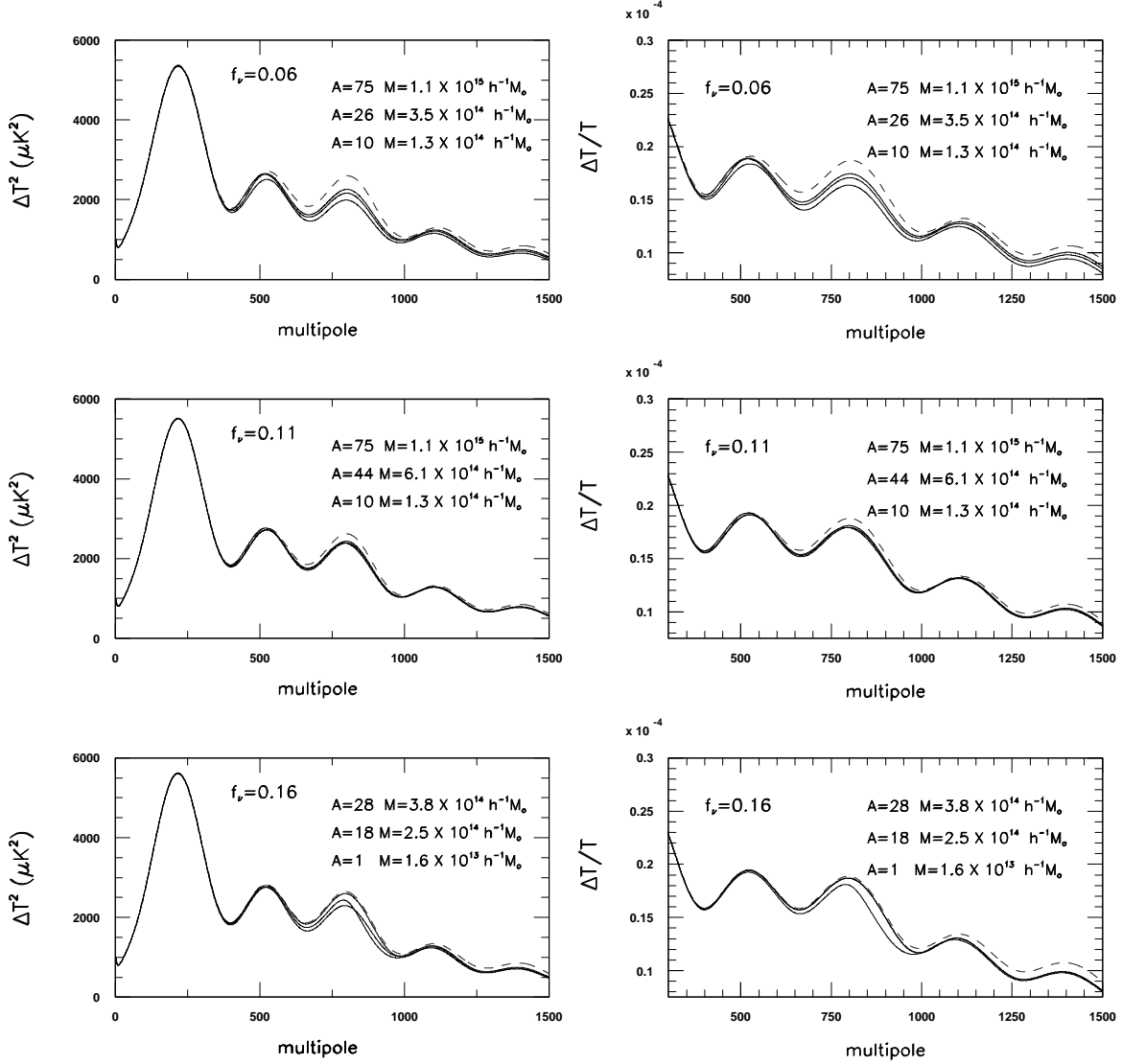


Fig. 8.— Left panels: the imprint of the neutrino gravitational clustering on the CMB anisotropy power spectrum obtained for the filtering perturbation with the mass M . Right panels: the CMB anisotropy $\Delta T/T$ computed in the presence of the gravitational clustering obtained for the filtering perturbation with the mass M . We report in the panels the richness of these perturbations. In each panel, the dashed line corresponds to the fiducial Λ CDM cosmological model, without including the effect of neutrino gravitational clustering, with $\Omega_m=0.38$, $\Omega_\Lambda=0.62$, $h=0.62$, $\tau=0.12$, $n_s=0.98$, three massive neutrino flavors and different neutrino fractions ($f_\nu=0.06, 0.011, 0.16$, from the top to the bottom). See also the text.

The characteristic angular scale left by the the neutrino gravitational clustering on the CMB anisotropy power spectrum is given by:

$$\theta = \frac{R_{fs}}{\eta_0 - \eta(a)}, \quad (8)$$

where R_{fs} is the scale of the filtering perturbation with the mass $M(R_{fs})$, $\eta(a)$ is the particle horizon distance at the time at which the non-linear perturbation mode k cross the horizon and η_0 is the particle horizon at the present time. Fig. 9 presents the evolution of the characteristic scale θ and of the corresponding multipole order of the CMB anisotropy power spectrum with the mass $M(R_{fs})$.

4. Imprints of neutrino gravitational clustering at PLANCK angular scales

The results presented in the previous section show that not only the high precision satellite experiments as MAP and PLANCK but also experiments as BOOMERANG, MAXIMA-1 and DASI have angular resolutions high enough to reveal the imprint of the neutrino gravitational clustering on the CMB angular power spectrum.

Of course, high sensitivity anisotropy measurements are necessary to determine the CMB angular power spectrum with an accuracy high enough to derive precise information on the main cosmological parameters and to be able of disentangle the imprint of neutrino gravitational clustering.

The cosmological parameter estimation from BOOMERANG data alone or with various combination of priors was reported by many authors (Bond et al. 2000, Lange et al 2001, Jaffe et al. 2001, Netterfield et al. 2001). All such limits must be understood in the context of the specific physical processes that one asks from the data. Inflation, justified by most of the experimental measurements in the field, predicts $\Omega_{tot} \simeq 1$ and a scalar spectral index

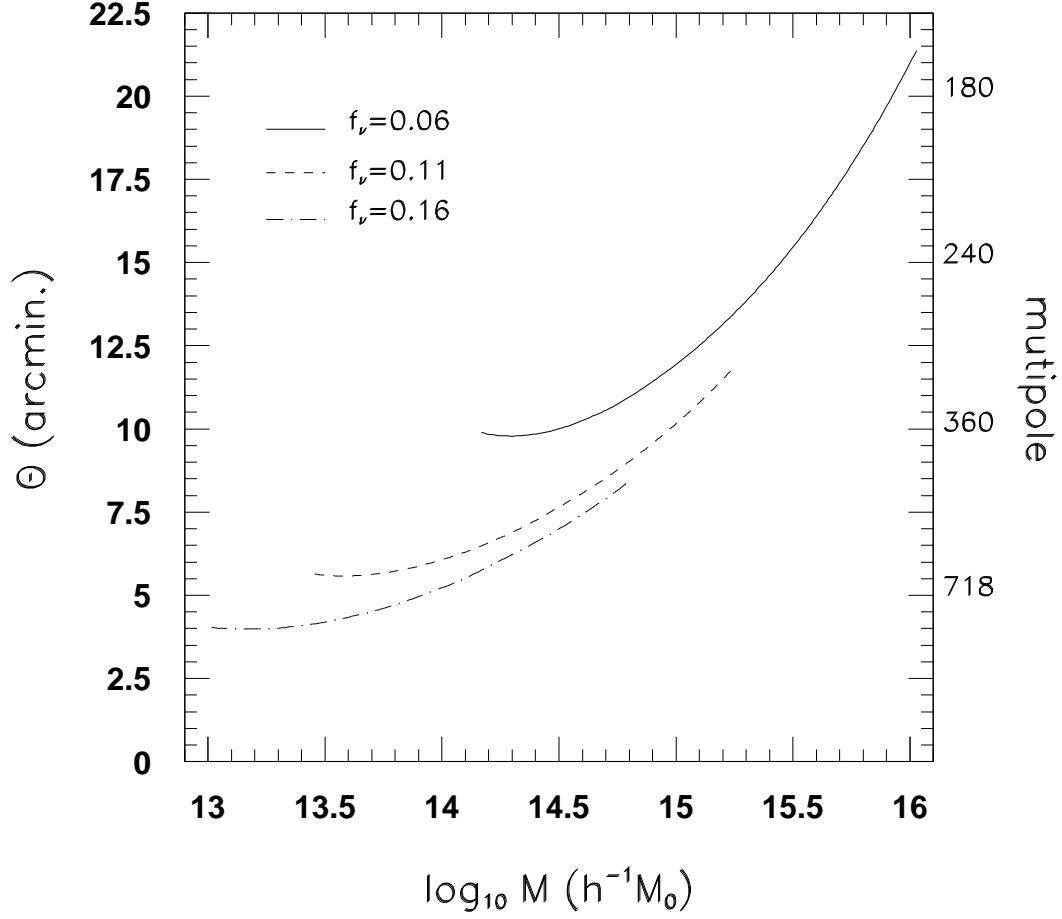


Fig. 9.— Evolution of the characteristic angular scale θ of the neutrino gravitational clustering with $M(R_{fs})$ for different neutrino fractions. We report also the corresponding multipole orders $l \sim \theta^{-1}$ of the CMB anisotropy power spectrum.

$n_s \simeq 1$.

Fig. 10 presents the BOOMERANG, MAXIMA-1 and DASI angular power spectra together with an inflation best fit model (Netterfield et al. 2001) obtained for BOOMERANG when priors from LSS are taken into account (Λ CDM model). In fact, current CMB anisotropy data, complemented with LSS data, can constrain Ω_m and Ω_b from the morphology of the Doppler peaks. The cosmological parameters of the considered best fit Λ CDM model are: $\Omega_{tot} = 1$, $\Omega_b h^2 = 0.021$, $\Omega_{cdm} h^2 = 0.13$, $\Omega_\Lambda = 0.62$, $\Omega_m = 0.37$, $\Omega_b = 0.05$, $h = 0.62$ and $\tau = 0.12$.

We make a simple likelihood analysis of the BOOMERANG, MAXIMA-1 and DASI measurements in order to see the extent to which these data sets can reveal cosmological information related to the neutrino gravitational clustering and to test the consistency among these data sets when the neutrino gravitational clustering is taken into account. Our computation is justified by the internal consistency found among these data sets once calibration, the systematic effects and beam uncertainties are taken into account (Wang, Tegmark & Zaldarriaga 2001).

For the BOOMERANG experiment, the most relevant systematic effect is the uncertainty in the beam width ($\delta\sigma_b = \Delta\text{FWHM}/\sqrt{8\ln 2} \simeq 1.4'/\sqrt{8\ln 2}$) while the calibration uncertainty, relevant for a combined analysis with other experiments, is of $\simeq 10\%$ ($1-\sigma$ errors; see Netterfield et al. 2001). We translate the beam width uncertainty to uncertainty on recovered CMB angular power spectrum by simply rescaling the beam window function, $\simeq \exp[-(\sigma_b \ell)^2]$. The MAXIMA-1 team directly provides the $1-\sigma$ errors on CMB angular power spectrum recovery introduced by the beam width uncertainty and pointing error, while the quoted $1-\sigma$ calibration error is $\simeq 8\%$ (Lee et al. 2001). The DASI angular power spectrum is affected by an uncertainty of $\simeq 2 - 4\%$ because of the errors in the estimated aperture efficiency and by a calibration uncertainty of $\simeq 7\%$ ($1-\sigma$ errors; see Halverson et al. 2001 and Leitch et al. 2001).

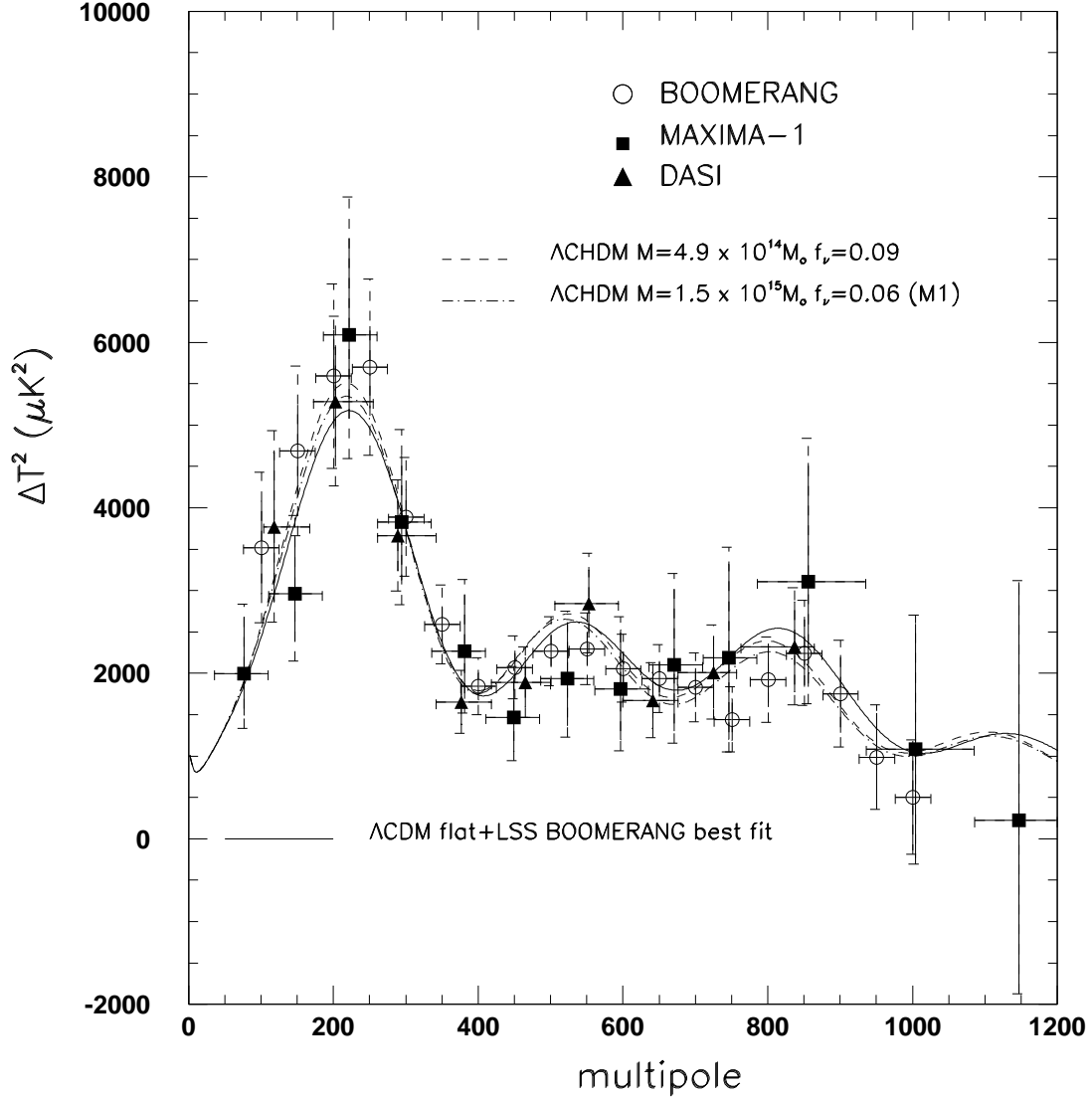


Fig. 10.— The CMB experimental power spectra from BOOMERANG, MAXIMA-1 and DASI experiments, the fiducial model and the best fit models in presence of the gravitational clustering. The dashed error bars include also the uncertainty due to systematics and calibration accuracy. See also the text.

A detailed analysis of the implications of these experiments including systematic effects is out of the scope of this work. We simply include the impact the systematic and calibration errors by computing upper and lower CMB angular power spectra by simply rescaling the nominal best fit (i.e. as quoted by the authors in absence these errors) angular power spectrum data by including the above multiplicative factor and by respectively adding or subtracting the statistic errors.

For this analysis we fix the parameters of our cosmological models to $\Omega_{tot} = 1$, $\Omega_m = 0.38$, $\Omega_\Lambda = 0.62$, $\Omega_b = 0.05$, $h = 0.62$, $n_s = 0.98$, $\tau = 0.12$ and add different fractions of three massive neutrino flavors f_ν in the range 0.001–0.17 (the neutrino total mass in the range 0.001–2 eV). We define a goodness of the fit as $-2\ln\mathcal{L}$ in terms of the likelihood function \mathcal{L} which reduces to the usual gaussian χ^2 . We find that BOOMERANG data are worst represented when neutrino a fraction is taken into account. In this case, the best fit is obtained for a neutrino fraction $f_\nu = 0.06 \pm 0.003$ ($m_\nu = 0.78 \pm 0.039$). We find an improvement of this fit when the neutrino gravitational clustering is taken into account, for a neutrino fraction $f_\nu = 0.06 \pm 0.003$ and an accreting mass of $M = 1.5 \times 10^{15} M_\odot$ that is closed to the mass of Coma cluster.

Fig. 11 presents the values of the reduced χ^2 obtained for different data sets and their combinations for the best fit cosmological model derived from BOOMERANG data. We also present the reduced χ^2 values obtained for a neutrino fraction $f_\nu = 0.09$ and an accreting mass $M = 4.9 \times 10^{14} M_\odot$, closed to the mass of the Abell cluster. The corresponding power spectra are plotted in Fig. 10. The likelihood values in Fig. 11 are obtained by taking into account the statistic and systematic errors. As expected, we find that the values of χ^2 are reduced (by a factor of about 1.5–2, according to the considered data set) when the calibration errors of the different experiments are also taken into account. On the other hand, the basic result remains the same: the smaller values of χ^2 are significantly

less dependent on the considered set of data when the neutrino gravitational clustering is included.

We have also computed the errors on the cosmological parameters by assuming as fiducial model the best fit derived from BOOMERANG data without clusterization with a neutrino fraction $f_\nu = 0.06$ (model M1) and the same model but including the neutrino gravitational clusterization with $f_\nu = 0.06$ and $M = 1.5 \times 10^{15} M_\odot$ (model M2) and considering the BOOMERANG data alone (B) and the combination of the data from BOOMERANG, MAXIMA and DASI (B+M+D). The result is presented in Tab. 2. We find that, in general, the errors on the cosmological parameters are smaller when the neutrino gravitational clusterization is taken into account.

In spite of the accuracy of current CMB anisotropy data, still quite poor to provide a firm detection of neutrino gravitational clusterization, and of the additional uncertainty represented by the relevant systematic effects, the above results indicate that including the neutrino gravitational clustering effect improves the consistency among BOOMERANG, MAXIMA-1 and DASI CMB angular power spectra, allowing in the same time a neutrino fraction in agreement with that indicated by the astroparticle and nuclear physics experiments and a cosmological accreting mass comparable with the mass of known clusters.

Clearly, new high sensitivity and resolution space anisotropy experiments will have a much better capability to detect the neutrino gravitational clustering effect. In particular, Planck will measure the CMB angular power spectrum with very high sensitivity up to multipoles $\ell \sim 1000 - 2000$ with a stringent control of the systematic effects.

Fig. 12 presents few confidence regions of the $f_\nu - M$ parameter space that can be potentially detected by PLANCK surveyor by using the CMB anisotropy measurements in the presence of the gravitational clustering. The target model used for this computation is the Λ CDM

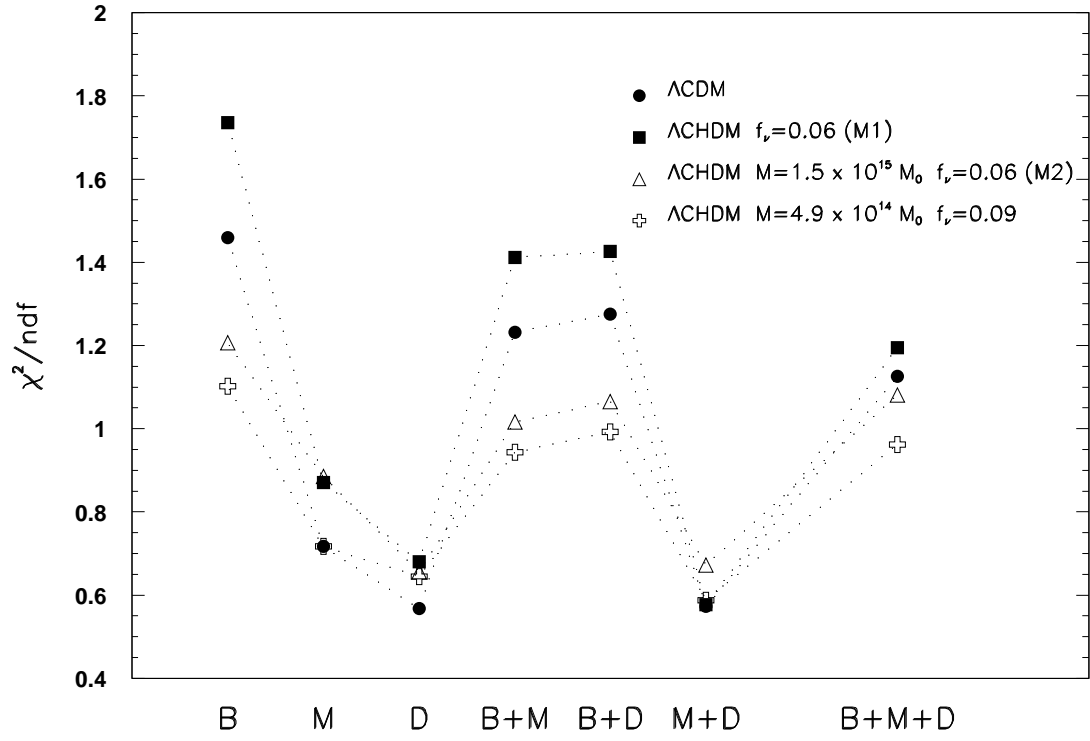


Fig. 11.— The reduced χ^2 obtained for BOOMERANG (B), MAXIMA-1 (M), DASI (D) and their combinations for the best fit cosmological models of BOOMERANG data. See also the text.

Table 2: $1\text{-}\sigma$ errors on the main cosmological parameters as obtained by using the Fisher information matrix taking the covariance matrix from BOOMERANG alone (B) and the covariance matrix of the combined BOOMERANG, MAXIMA-1 and DASI experiments (B+M+D). Model M1: data represented by the Λ CHDM model with $f_\nu = 0.06$ by neglecting the effect of clustering. Model M2: data represented by the Λ CHDM model with $f_\nu = 0.06$ by including the clustering effect assuming $M = 1.5 \times 10^{15} M_\odot$. For the case of B+M+D the covariance matrix was obtained taking into account the systematic errors and the calibration errors (as indicated in the table).

Experiment	Model	n_s	τ	$\Omega_b h^2$	$\Omega_c h^2$	$\Omega_\nu h^2$	Ω_m	Ω_Λ	h
B	M1	0.083	0.049	0.0031	0.039	0.0045	0.098	0.081	0.087
B	M2	0.058	0.021	0.0025	0.026	0.0028	0.081	0.053	0.042
B+M+D ^{sy}	M1	0.069	0.043	0.0029	0.034	0.0039	0.097	0.047	0.051
B+M+D ^{sy}	M2	0.051	0.027	0.0026	0.022	0.0018	0.071	0.044	0.036
B+M+D ^{cal}	M1	0.101	0.071	0.0037	0.057	0.0064	0.141	0.069	0.076
B+M+D ^{cal}	M2	0.089	0.058	0.0031	0.038	0.0031	0.112	0.058	0.062

model best fit of the BOOMERANG data. We fix the parameters of our cosmological models to $\Omega_{tot} = 1$, $\Omega_m = 0.38$, $\Omega_\Lambda = 0.62$, $\Omega_b = 0.05$, $h = 0.62$, $n_s = 0.98$, $\tau = 0.12$ and compute the CMB anisotropy power spectra adding different fractions of three massive neutrino flavors f_ν in the range 0.001–0.1 (the neutrino total mass in the range 0.001–1.3 eV), for different values of the accreting mass in the range $5 \times 10^{14} - 5 \times 10^{15} h^{-1} M_\odot$.

We consider for this computation only the PLANCK “cosmological” channel between 70 and 217 GHz, a sky coverage $f_{sky} = 0.8$ and neglect for simplicity the foreground contamination (see Popa, Burigana & Mandolesi 2001 and references therein).

At 68% confidence level we obtain a neutrino fraction $f_\nu \approx 0.011 \pm 0.007$ for an accreting mass $M \approx (8.2 \pm 3.1) \times 10^{14} h^{-1} M_\odot$. Fig. 11 shows that PLANCK surveyor will have the capability to measure the imprints of the neutrino gravitational clustering on the CMB anisotropy power spectrum for a neutrino mass range in agreement with that indicated by the astroparticle and nuclear physics experiments and a cosmological accreting mass comparable with the mass of the known clusters.

5. Conclusions

In this paper we study the CMB anisotropy induced by the non-linear perturbations in the massive neutrino density associated to the non-linear gravitational clustering. Through numerical simulations, we compute the CMB anisotropy angular power spectrum in the non-linear stages of the evolution of the universe when clusters and superclusters start to form, producing a non-linear time varying gravitational potential. Motivated by the consistency with the LSS data and the latest CMB anisotropy measurements, our cosmological model is a flat Λ CDM model with different neutrino fractions f_ν corresponding to a neutrino total mass in the range allowed by the neutrino oscillation and double beta decay experiments.

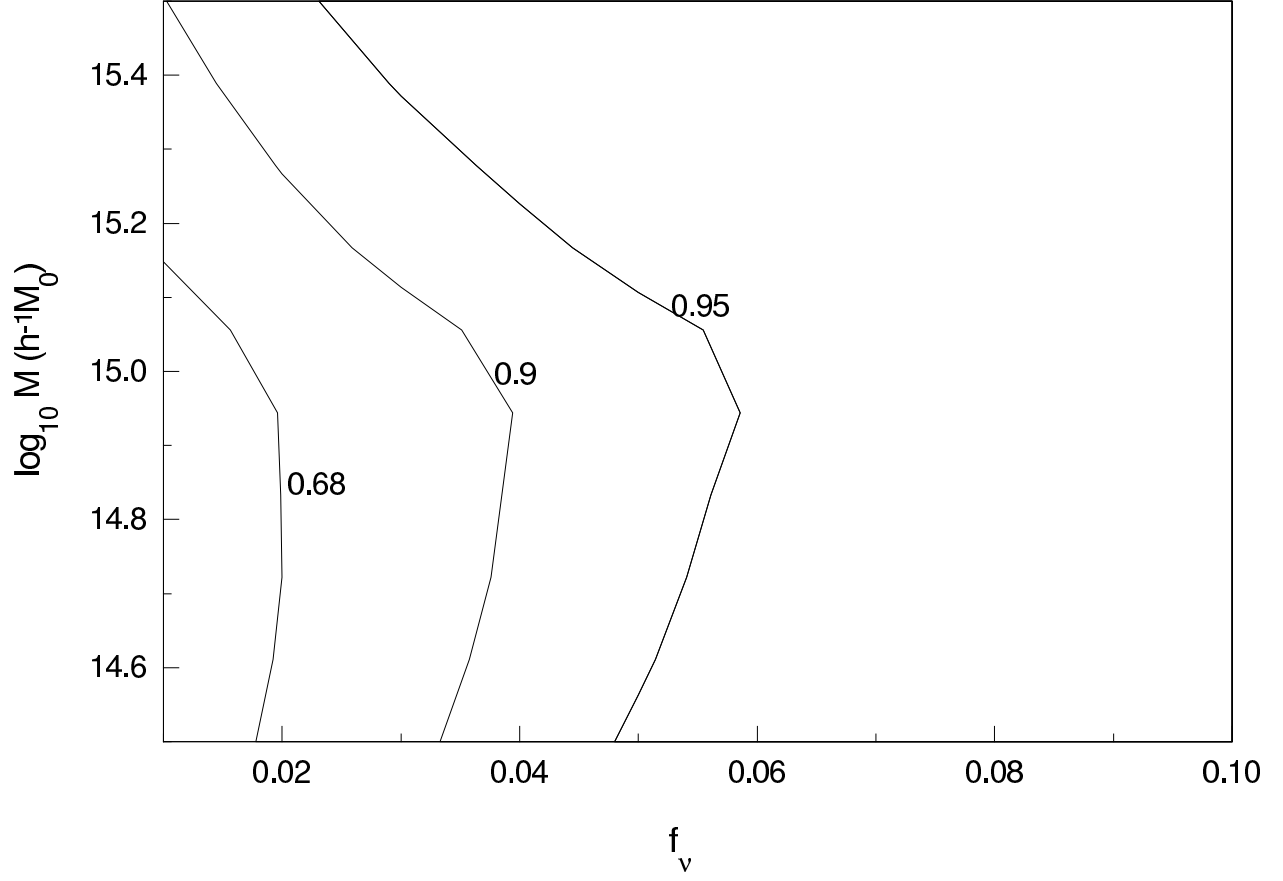


Fig. 12.— Confidence regions of the f_ν - M parameter space that can be potentially detected by PLANCK surveyor by using the CMB anisotropy measurements in the presence of the gravitational clustering.

We compute the imprint left by the gravitational clustering on the CMB anisotropy power spectrum for all non-linear scales, taking into account the time evolution of all non-linear density perturbations in a large simulation box (with the size of 128 Mpc) encompassing the comoving horizon size at matter-radiation equality and a large simulated mass (the total mass of $\sim 5 \times 10^{18} M_{\odot}$) that ensures that our simulation is a fair sample of the matter evolution in the non-linear stages.

We found that the non-linear time varying potential induced by the gravitational clustering process generates metric perturbations that affect the time evolution of the density fluctuations in all the components of the expanding universe, leaving imprints on the CMB anisotropy power spectrum at subdegree angular scales. The magnitude of the induced anisotropy and the characteristic angular scale depends on how each non-linear mode k of the perturbations relates to the neutrino free-streaming wavenumber k_{fs} at each evolution time step. By smoothing the density field obtained from simulations with a filter with the scale corresponding to the cluster scale, we find an imprint on the CMB anisotropy power spectrum of amplitude $\Delta T/T \approx 10^{-6}$ for angular resolutions between ~ 4 and 20 arcminutes, depending on the cluster mass and neutrino fraction f_{ν} .

This result suggests that the CMB anisotropy experiments with such levels of sensitivities and angular resolutions should detect the dynamical effect of the non-linear gravitational clustering.

We analyzed the consistency among BOOMERANG, MAXIMA-1 and DASI anisotropy measurements when the non-linear effects induced by the gravitational clustering are taken into account. Our results suggest that including the neutrino gravitational clustering effect improves the consistency among BOOMERANG, MAXIMA-1 and DASI CMB angular power spectra and the errors on most of the cosmological parameters. For a neutrino fraction in agreement with that indicated by the astroparticle and nuclear physics experiments and a cosmological accreting mass comparable with the mass of known the clusters, we find that

the PLANCK angular resolution and sensitivity will allow the detection of the dynamical effects of the gravitational clustering from the CMB anisotropy measurements.

It is a pleasure to thank U. Seljak and M. Zaldarriaga for the use of the CMBFAST code (v3.2) employed in the computation of the CMB power spectrum and of the matter transfer function.

REFERENCES

- Aghanim, N., Desert, F.X., Puget, J.L., Gispert, R., 1996, A&A, astro-ph/9604083
- Ambrosio, M., Atolini, R., Arano, C., et al. (MACRO Collab.), 1998, Phys. Lett. B, 434, 451
- Bardeen, J.M., 1980, Phys. Rev. D22, 1882
- Bertschinger, E., 1995, [http : //arcturus.mit.edu/cosmics](http://arcturus.mit.edu/cosmics)
- Blanchard, A. & Schneider, J. 1987, A&A 184, 1
- Bond, J.R., Efstathiou, G. & Silk, J. 1980, Phys. rev. Lett. 45, 1980
- Bond, J.R., Szalay, A.S., 1983, ApJ 274, 443
- Bond, J.R., et al. 2000, astro-ph/0011378
- Cole, S. & Efstathiou, G. 1989, MNRAS 239, 195
- Dodelson, S., Gates, E. & Stebbins, A., 1996, ApJ 467, 10
- Eke, V.R., Cole, S., Frenk, C.S., 1996, MNRAS, 282, 263
- Efstathiou, G., Bridle, S.L., Lasenby, A.N., et al., 1999, MNRAS, 303, L47-52
- Efstathiou, G., Eastwood, J.W., 1981, MNRAS, 194, 503
- Freese, K., Kolb, E.W. & Turner, M., 1983 Phys. Rev. D 27, 1689
- Fukuda, Y., Hayakawa, T., Ichihara, E., et al. (Super-Kamiokande Collab.), 1998, Phys. Rev. Lett., 81, 1562
- Fukugita, M., Liu, G.C., Sugiyama, N., 1999, Phys. Rev. Lett., 84, 1082

- Ganon, G., Hoffman, Y., 1993, ApJL, 415, 5
- Gawiser, E., Silk, J., 1998, Science 280, 1405
- Gleb, J., Bertshinger, E., 1994, ApJ 436, 467
- Gruzinov, A. & Hu, W. 1988, ApJ 508, 435
- Halverson, N.W., Leitch, E.M., Pryke, C., et al., 2001, astro-ph/0104489
- Hancock, S., Rocha, G., Lasenby, A.N., et al., 1998, MNRAS, 294, L1
- Hockney, R.W., Eastwood, J.W., 1981, Computer Simulations Using Particles (New York: McGraw-Hill)
- Hoffman, Y., Ribak, R., 1991, ApJL, 380, 5
- Hu, W., Eisenstein, D.J., 1998, ApJ, 498, 497
- Hu, W. & Sugiyama, N., 1995, ApJ 444, 489
- Hu, W., Sugiyama, N. & Silk, J. 1997, Nature 386, 37
- Jaffe, A., et al. 2001, Phys. Rev. Lett., 86, 3475
- Kashlinsky, A., 1998, ApJ 492, 1
- Kates, R., Kotok, E. & Klypin, E., 1991, A&A 243, 295
- Klapdor-Kleingrothaus, H.V. 2001, Nuclear Phys. B 100, 309
- Klypin, A. & Holtzman, J., 1997, astro-ph/9712217
- Kodama, H. & Sasaki, M., 1984, Prog. Theor. Phys. Suppl. 78, 1
- Kofman, L.A. & Starobinskii, A.A. 1985, Sov. Astron. Lett. 434, L1-L4

- Kolb, W.E. & Turner, M., 1990 in *The Early Universe* (Addison-Wesley Publishing)
- Lange, A.E., et al. 2001, *Phys. Rev. D* 63, 042001
- Lee, A.T., Ade, P., Balbi, A., et al., 2001, *ApJ* 561, L1-L6
- Leitch, E.M., Pryke, C., Halverson, N.W., et al., 2001, *ApJ* 561, L1-L6
- Ma, C.P., *ApJ*, 1996, 471, 13
- Ma, C.P., 2000, in *Neutrinos in Physics and Astrophysics: From 10^{-33} to 10^{28} cm*, ed. Paul Langacker (Singapore:World Scientific), 504
- Ma, C.P., Bertschinger, E., 1995, *ApJ*, 455, 7
- Magliocchetti, M., Moscardini, L., Panuzzo, P., Granato, G.L., De Zotti, G., Danese, L., 2001, *MNRAS*, in press, astro-ph/0102464
- Martinez-Gonzalez, E. & Sanz, J., 1992, *PRD* 46, 4193
- Mather, J.C., et al. *ApJ* 512, 511
- Netterfield, C.B., Ade, P.A.R., Bock, J.J., et al., 2001, astro-ph/0104460
- Ostriker, J.P. & Vishniac, E.T., 1986, *ApJ Lett.* 306, L51-L58
- Padin, S., et al. 2001, *ApJL* 549, L1
- Peacock, A.J., 2000, in *Cosmological Physics* (Cambridge: University Press)
- Perlmutter S., Aldering G., Deustua S., et al., 1997, *Bull. Am. Astron. Soc.*, 29, 1351
- Popa, L.A., Burigana, C. & Mandolesi N., 2001, *ApJ* 558, 10
- Primack, J.R. & Gross, A.K., 2000, in *Current Aspects of Neutrino Physics*, ed. Caldwell, D.O. (Springer, Berlin Heidelberg)

- Primack, R.J., Holtzman, J., Klypin, A., Caldwell, D.O., 1995, Phys. Rev. Lett., 74, 12
- Quilis, V., Ibanez, J.M. & Saez. D., 1995, MNRAS, astro-ph/9507019 v2
- Rees, M.J. & Sciama, D.N. 1968, Nature, 519
- Riess, A.G., Filippenko, A.V, Challis, P., et al., 1998, AJ, 116, 1009
- Scott, D., White, M., 1994, in the Proceedings of the CWRU CMB Workshop “2 Years after COBE”, eds. L. M. Krauss, P.(Singapore: Worls Scientific), 142
- Seljak, U., Zaldarriaga, M., 1996, ApJ, 469, 437
- Sunyaev, R.A. & Zel’dovich, Ya. B., 1972, Comm. Astrophys. Space Phys. 4 173
- Tremaine, S. & Gunn, J.E. 1979, Phys. Rev. Lett. 42, 407
- Vishniac, E.T. 1987, ApJ 322, 597
- Wang,X., Tegmark, M. & Zaldarriaga, M. 2001, astro-ph/0105091 v3
- White, M., Gelmini, G., Silk, J., 1995, PRD, 51, 2669
- Zel’dovich, Ya.B., 1970, A&A, 5, 84